Direct Measurement of the W Production Charge Asymmetry in $p\bar{p}$ Collisions at $\sqrt{s} = 1.96$ TeV

T. Aaltonen,[24] J. Adelman,[14] T. Akimoto,[56] B. Álvarez González[s],[12] S. Amerio[y],[44] D. Amidei,[35] A. Anastassov,[39] A. Annovi,[20] J. Antos,[15] G. Apollinari,[18] A. Apresyan,[49] T. Arisawa,[58] A. Artikov,[16] W. Ashmanskas,[18] A. Attal,[4] A. Aurisano,[54] F. Azfar,[43] P. Azzurri[z],[47] W. Badgett,[18] A. Barbaro-Galtieri,[29] V.E. Barnes,[49] B.A. Barnett,[26] V. Bartsch,[31] G. Bauer,[33] P.-H. Beauchemin,[34] F. Bedeschi,[47] D. Beecher,[31] S. Behari,[26] G. Bellettini[z],[47] J. Bellinger,[60] D. Benjamin,[17] A. Beretvas,[18] J. Beringer,[29] A. Bhatti,[51] M. Binkley,[18] D. Bisello[y],[44] I. Bizjak[ee],[31] R.E. Blair,[2] C. Blocker,[7] B. Blumenfeld,[26] A. Bocci,[17] A. Bodek,[50] V. Boisvert,[50] G. Bolla,[49] D. Bortoletto,[49] J. Boudreau,[48] A. Boveia,[11] B. Brau[a],[11] A. Bridgeman,[25] L. Brigliadori,[44] C. Bromberg,[36] E. Brubaker,[14] J. Budagov,[16] H.S. Budd,[50] S. Budd,[25] S. Burke,[18] K. Burkett,[18] G. Busetto[y],[44] P. Bussey,[22] A. Buzatu,[34] K. L. Byrum,[2] S. Cabrera[u],[17] C. Calancha,[32] M. Campanelli,[36] M. Campbell,[35] F. Canelli[14],[18] A. Canepa,[46] B. Carls,[25] D. Carlsmith,[60] R. Carosi,[47] S. Carrillo[n],[19] S. Carron,[34] B. Casal,[12] M. Casarsa,[18] A. Castro[x],[6] P. Catastini[aa],[47] D. Cauz[dd],[55] V. Cavaliere[aa],[47] M. Cavalli-Sforza,[4] A. Cerri,[29] L. Cerrito[o],[31] S.H. Chang,[28] Y.C. Chen,[1] M. Chertok,[8] G. Chiarelli,[47] G. Chlachidze,[18] F. Chlebana,[18] K. Cho,[28] D. Chokheli,[16] J.P. Chou,[23] G. Choudalakis,[33] S.H. Chuang,[53] K. Chung,[13] W.H. Chung,[60] Y.S. Chung,[50] T. Chwalek,[27] C.I. Ciobanu,[45] M.A. Ciocci[aa],[47] A. Clark,[21] D. Clark,[7] G. Compostella,[44] M.E. Convery,[18] J. Conway,[8] M. Cordelli,[20] G. Cortiana[y],[44] C.A. Cox,[8] D.J. Cox,[8] F. Crescioli[z],[47] C. Cuenca Almenar[u],[8] J. Cuevas[s],[12] R. Culbertson,[18] J.C. Cully,[35] D. Dagenhart,[18] M. Datta,[18] T. Davies,[22] P. de Barbaro,[50] S. De Cecco,[52] A. Deisher,[29] G. De Lorenzo,[4] M. Dell'Orso[z],[47] C. Deluca,[4] L. Demortier,[51] J. Deng,[17] M. Deninno,[6] P.F. Derwent,[18] G.P. di Giovanni,[45] C. Dionisi[cc],[52] B. Di Ruzza[dd],[55] J.R. Dittmann,[5] M. D'Onofrio,[4] S. Donati[z],[47] P. Dong,[9] J. Donini,[44] T. Dorigo,[44] S. Dube,[53] J. Efron,[40] A. Elagin,[54] R. Erbacher,[8] D. Errede,[25] S. Errede,[25] R. Eusebi,[18] H.C. Fang,[29] S. Farrington,[43] W.T. Fedorko,[14] R.G. Feild,[61] M. Feindt,[27] J.P. Fernandez,[32] C. Ferrazza[bb],[47] R. Field,[19] G. Flanagan,[49] R. Forrest,[8] M.J. Frank,[5] M. Franklin,[23] J.C. Freeman,[18] I. Furic,[19] M. Gallinaro,[52] J. Galyardt,[13] F. Garberson,[11] J.E. Garcia,[21] A.F. Garfinkel,[49] K. Genser,[18] H. Gerberich,[25] D. Gerdes,[35] A. Gessler,[27] S. Giagu[cc],[52] V. Giakoumopoulou,[3] P. Giannetti,[47] K. Gibson,[48] J.L. Gimmell,[50] C.M. Ginsburg,[18] N. Giokaris,[3] M. Giordani[dd],[55] P. Giromini,[20] M. Giunta[z],[47] G. Giurgiu,[26] V. Glagolev,[16] D. Glenzinski,[18] M. Gold,[38] N. Goldschmidt,[19] A. Golossanov,[18] G. Gomez,[12] G. Gomez-Ceballos,[33] M. Goncharov,[33] O. González,[32] I. Gorelov,[38] A.T. Goshaw,[17] K. Goulianos,[51] A. Gresele[y],[44] S. Grinstein,[23] C. Grosso-Pilcher,[14] R.C. Group,[18] U. Grundler,[25] J. Guimaraes da Costa,[23] Z. Gunay-Unalan,[36] C. Haber,[29] K. Hahn,[33] S.R. Hahn,[18] E. Halkiadakis,[53] B.-Y. Han,[50] J.Y. Han,[50] F. Happacher,[20] K. Hara,[56] D. Hare,[53] M. Hare,[57] S. Harper,[43] R.F. Harr,[59] R.M. Harris,[18] M. Hartz,[48] K. Hatakeyama,[51] C. Hays,[43] M. Heck,[27] A. Heijboer,[46] J. Heinrich,[46] C. Henderson,[33] M. Herndon,[60] J. Heuser,[27] S. Hewamanage,[5] D. Hidas,[17] C.S. Hill[c],[11] D. Hirschbuehl,[27] A. Hocker,[18] S. Hou,[1] M. Houlden,[30] S.-C. Hsu,[29] B.T. Huffman,[43] R.E. Hughes,[40] U. Husemann,[61] M. Hussein,[36] J. Huston,[36] J. Incandela,[11] G. Introzzi,[47] M. Iori[cc],[52] A. Ivanov,[8] E. James,[18] D. Jang,[13] B. Jayatilaka,[17] E.J. Jeon,[28] M.K. Jha,[6] S. Jindariani,[18] W. Johnson,[8] M. Jones,[49] K.K. Joo,[28] S.Y. Jun,[13] J.E. Jung,[28] T.R. Junk,[18] T. Kamon,[54] D. Kar,[19] P.E. Karchin,[59] Y. Kato[l],[42] R. Kephart,[18] J. Keung,[46] V. Khotilovich,[54] B. Kilminster,[18] D.H. Kim,[28] H.S. Kim,[28] H.W. Kim,[28] J.E. Kim,[28] M.J. Kim,[20] S.B. Kim,[28] S.H. Kim,[56] Y.K. Kim,[14] N. Kimura,[56] L. Kirsch,[7] S. Klimenko,[19] B. Knuteson,[33] B.R. Ko,[17] K. Kondo,[58] D.J. Kong,[28] J. Konigsberg,[19] A. Korytov,[19] A.V. Kotwal,[17] M. Kreps,[27] J. Kroll,[46] D. Krop,[14] N. Krumnack,[5] M. Kruse,[17] V. Krutelyov,[11] T. Kubo,[56] T. Kuhr,[27] N.P. Kulkarni,[59] M. Kurata,[56] S. Kwang,[14] A.T. Laasanen,[49] S. Lami,[47] S. Lammel,[18] M. Lancaster,[31] R.L. Lander,[8] K. Lannon[r],[40] A. Lath,[53] G. Latino[aa],[47] I. Lazzizzera[y],[44] T. LeCompte,[2] E. Lee,[54] H.S. Lee,[14] S.W. Lee[t],[54] S. Leone,[47] J.D. Lewis,[18] C.-S. Lin,[29] J. Linacre,[43] M. Lindgren,[18] E. Lipeles,[46] A. Lister,[8] D.O. Litvintsev,[18] C. Liu,[48] T. Liu,[18] N.S. Lockyer,[46] A. Loginov,[61] M. Loreti[y],[44] L. Lovas,[15] D. Lucchesi[y],[44] C. Luci[cc],[52] J. Lueck,[27] P. Lujan,[29] P. Lukens,[18] G. Lungu,[51] L. Lyons,[43] J. Lys,[29] R. Lysak,[15] D. MacQueen,[34] R. Madrak,[18] K. Maeshima,[18] K. Makhoul,[33] T. Maki,[24] P. Maksimovic,[26] S. Malde,[43] S. Malik,[31] G. Manca[e],[30] A. Manousakis-Katsikakis,[3] F. Margaroli,[49] C. Marino,[27] C.P. Marino,[25] A. Martin,[61] V. Martin[k],[22] M. Martínez,[4] R. Martínez-Ballarín,[32] T. Maruyama,[56] P. Mastrandrea,[52] T. Masubuchi,[56] M. Mathis,[26] M.E. Mattson,[59] P. Mazzanti,[6] K.S. McFarland,[50] P. McIntyre,[54] R. McNulty[j],[30] A. Mehta,[30] P. Mehtala,[24] A. Menzione,[47] P. Merkel,[49] C. Mesropian,[51] T. Miao,[18] N. Miladinovic,[7] R. Miller,[36] C. Mills,[23] M. Milnik,[27] A. Mitra,[1] G. Mitselmakher,[19] H. Miyake,[56] N. Moggi,[6] C.S. Moon,[28] R. Moore,[18] M.J. Morello[z],[47]

J. Morlock,[27] P. Movilla Fernandez,[18] J. Mülmenstädt,[29] A. Mukherjee,[18] Th. Muller,[27] R. Mumford,[26] P. Murat,[18] M. Mussini[x],[6] J. Nachtman,[18] Y. Nagai,[56] A. Nagano,[56] J. Naganoma,[56] K. Nakamura,[56] I. Nakano,[41] A. Napier,[57] V. Necula,[17] J. Nett,[60] C. Neu[v],[46] M.S. Neubauer,[25] S. Neubauer,[27] J. Nielsen[g],[29] L. Nodulman,[2] M. Norman,[10] O. Norniella,[25] E. Nurse,[31] L. Oakes,[43] S.H. Oh,[17] Y.D. Oh,[28] I. Oksuzian,[19] T. Okusawa,[42] R. Orava,[24] K. Osterberg,[24] S. Pagan Griso[y],[44] E. Palencia,[18] V. Papadimitriou,[18] A. Papaikonomou,[27] A.A. Paramonov,[14] B. Parks,[40] S. Pashapour,[34] J. Patrick,[18] G. Pauletta[dd],[55] M. Paulini,[13] C. Paus,[33] T. Peiffer,[27] D.E. Pellett,[8] A. Penzo,[55] T.J. Phillips,[17] G. Piacentino,[47] E. Pianori,[46] L. Pinera,[19] K. Pitts,[25] C. Plager,[9] L. Pondrom,[60] O. Poukhov[*],[16] N. Pounder,[43] F. Prakoshyn,[16] A. Pronko,[18] J. Proudfoot,[2] F. Ptohos[i],[18] E. Pueschel,[13] G. Punzi[z],[47] J. Pursley,[60] J. Rademacker[c],[43] A. Rahaman,[48] V. Ramakrishnan,[60] N. Ranjan,[49] I. Redondo,[32] P. Renton,[43] M. Renz,[27] M. Rescigno,[52] S. Richter,[27] F. Rimondi[x],[6] L. Ristori,[47] A. Robson,[22] T. Rodrigo,[12] T. Rodriguez,[46] E. Rogers,[25] S. Rolli,[57] R. Roser,[18] M. Rossi,[55] R. Rossin,[11] P. Roy,[34] A. Ruiz,[12] J. Russ,[13] V. Rusu,[18] B. Rutherford,[18] H. Saarikko,[24] A. Safonov,[54] W.K. Sakumoto,[50] O. Saltó,[4] L. Santi[dd],[55] S. Sarkar[cc],[52] L. Sartori,[47] K. Sato,[18] A. Savoy-Navarro,[45] P. Schlabach,[18] A. Schmidt,[27] E.E. Schmidt,[18] M.A. Schmidt,[14] M.P. Schmidt[*],[61] M. Schmitt,[39] T. Schwarz,[8] L. Scodellaro,[12] A. Scribano[aa],[47] F. Scuri,[47] A. Sedov,[49] S. Seidel,[38] Y. Seiya,[42] A. Semenov,[16] L. Sexton-Kennedy,[18] F. Sforza,[47] A. Sfyrla,[25] S.Z. Shalhout,[59] T. Shears,[30] P.F. Shepard,[48] M. Shimojima[q],[56] S. Shiraishi,[14] M. Shochet,[14] Y. Shon,[60] I. Shreyber,[37] A. Sidoti,[47] P. Sinervo,[34] A. Sisakyan,[16] A.J. Slaughter,[18] J. Slaunwhite,[40] K. Sliwa,[57] J.R. Smith,[8] F.D. Snider,[18] R. Snihur,[34] A. Soha,[8] S. Somalwar,[53] V. Sorin,[36] J. Spalding,[18] T. Spreitzer,[34] P. Squillacioti[aa],[47] M. Stanitzki,[61] R. St. Denis,[22] B. Stelzer,[34] O. Stelzer-Chilton,[34] D. Stentz,[39] J. Strologas,[38] G.L. Strycker,[35] D. Stuart,[11] J.S. Suh,[28] A. Sukhanov,[19] I. Suslov,[16] T. Suzuki,[56] A. Taffard[f],[25] R. Takashima,[41] Y. Takeuchi,[56] R. Tanaka,[41] M. Tecchio,[35] P.K. Teng,[1] K. Terashi,[51] J. Thom[h],[18] A.S. Thompson,[22] G.A. Thompson,[25] E. Thomson,[46] P. Tipton,[61] P. Ttito-Guzmán,[32] S. Tkaczyk,[18] D. Toback,[54] S. Tokar,[15] K. Tollefson,[36] T. Tomura,[56] D. Tonelli,[18] S. Torre,[20] D. Torretta,[18] P. Totaro[dd],[55] S. Tourneur,[45] M. Trovato,[47] S.-Y. Tsai,[1] Y. Tu,[46] N. Turini[aa],[47] F. Ukegawa,[56] S. Vallecorsa,[21] N. van Remortel[b],[24] A. Varganov,[35] E. Vataga[bb],[47] F. Vázquez[n],[19] G. Velev,[18] C. Vellidis,[3] M. Vidal,[32] R. Vidal,[18] I. Vila,[12] R. Vilar,[12] T. Vine,[31] M. Vogel,[38] I. Volobouev[t],[29] G. Volpi[z],[47] P. Wagner,[46] R.G. Wagner,[2] R.L. Wagner,[18] W. Wagner[w],[27] J. Wagner-Kuhr,[27] T. Wakisaka,[42] R. Wallny,[9] S.M. Wang,[1] A. Warburton,[34] D. Waters,[31] M. Weinberger,[54] J. Weinelt,[27] W.C. Wester III,[18] B. Whitehouse,[57] D. Whiteson[f],[46] A.B. Wicklund,[2] E. Wicklund,[18] S. Wilbur,[14] G. Williams,[34] H.H. Williams,[46] P. Wilson,[18] B.L. Winer,[40] P. Wittich[h],[18] S. Wolbers,[18] C. Wolfe,[14] T. Wright,[35] X. Wu,[21] F. Würthwein,[10] S. Xie,[33] A. Yagil,[10] K. Yamamoto,[42] J. Yamaoka,[17] U.K. Yang[p],[14] Y.C. Yang,[28] W.M. Yao,[29] G.P. Yeh,[18] J. Yoh,[18] K. Yorita,[58] T. Yoshida[m],[42] G.B. Yu,[50] I. Yu,[28] S.S. Yu,[18] J.C. Yun,[18] L. Zanello[cc],[52] A. Zanetti,[55] X. Zhang,[25] Y. Zheng[d],[9] and S. Zucchelli[x],[6]

(CDF Collaboration[†])

[1]*Institute of Physics, Academia Sinica, Taipei, Taiwan 11529, Republic of China*
[2]*Argonne National Laboratory, Argonne, Illinois 60439*
[3]*University of Athens, 157 71 Athens, Greece*
[4]*Institut de Fisica d'Altes Energies, Universitat Autonoma de Barcelona, E-08193, Bellaterra (Barcelona), Spain*
[5]*Baylor University, Waco, Texas 76798*
[6]*Istituto Nazionale di Fisica Nucleare Bologna, [x]University of Bologna, I-40127 Bologna, Italy*
[7]*Brandeis University, Waltham, Massachusetts 02254*
[8]*University of California, Davis, Davis, California 95616*
[9]*University of California, Los Angeles, Los Angeles, California 90024*
[10]*University of California, San Diego, La Jolla, California 92093*
[11]*University of California, Santa Barbara, Santa Barbara, California 93106*
[12]*Instituto de Fisica de Cantabria, CSIC-University of Cantabria, 39005 Santander, Spain*
[13]*Carnegie Mellon University, Pittsburgh, PA 15213*
[14]*Enrico Fermi Institute, University of Chicago, Chicago, Illinois 60637*
[15]*Comenius University, 842 48 Bratislava, Slovakia; Institute of Experimental Physics, 040 01 Kosice, Slovakia*
[16]*Joint Institute for Nuclear Research, RU-141980 Dubna, Russia*
[17]*Duke University, Durham, North Carolina 27708*
[18]*Fermi National Accelerator Laboratory, Batavia, Illinois 60510*
[19]*University of Florida, Gainesville, Florida 32611*
[20]*Laboratori Nazionali di Frascati, Istituto Nazionale di Fisica Nucleare, I-00044 Frascati, Italy*
[21]*University of Geneva, CH-1211 Geneva 4, Switzerland*
[22]*Glasgow University, Glasgow G12 8QQ, United Kingdom*
[23]*Harvard University, Cambridge, Massachusetts 02138*

[24]Division of High Energy Physics, Department of Physics,
University of Helsinki and Helsinki Institute of Physics, FIN-00014, Helsinki, Finland
[25]University of Illinois, Urbana, Illinois 61801
[26]The Johns Hopkins University, Baltimore, Maryland 21218
[27]Institut für Experimentelle Kernphysik, Universität Karlsruhe, 76128 Karlsruhe, Germany
[28]Center for High Energy Physics: Kyungpook National University,
Daegu 702-701, Korea; Seoul National University, Seoul 151-742,
Korea; Sungkyunkwan University, Suwon 440-746,
Korea; Korea Institute of Science and Technology Information, Daejeon,
305-806, Korea; Chonnam National University, Gwangju, 500-757, Korea
[29]Ernest Orlando Lawrence Berkeley National Laboratory, Berkeley, California 94720
[30]University of Liverpool, Liverpool L69 7ZE, United Kingdom
[31]University College London, London WC1E 6BT, United Kingdom
[32]Centro de Investigaciones Energeticas Medioambientales y Tecnologicas, E-28040 Madrid, Spain
[33]Massachusetts Institute of Technology, Cambridge, Massachusetts 02139
[34]Institute of Particle Physics: McGill University, Montréal, Québec,
Canada H3A 2T8; Simon Fraser University, Burnaby, British Columbia,
Canada V5A 1S6; University of Toronto, Toronto, Ontario,
Canada M5S 1A7; and TRIUMF, Vancouver, British Columbia, Canada V6T 2A3
[35]University of Michigan, Ann Arbor, Michigan 48109
[36]Michigan State University, East Lansing, Michigan 48824
[37]Institution for Theoretical and Experimental Physics, ITEP, Moscow 117259, Russia
[38]University of New Mexico, Albuquerque, New Mexico 87131
[39]Northwestern University, Evanston, Illinois 60208
[40]The Ohio State University, Columbus, Ohio 43210
[41]Okayama University, Okayama 700-8530, Japan
[42]Osaka City University, Osaka 588, Japan
[43]University of Oxford, Oxford OX1 3RH, United Kingdom
[44]Istituto Nazionale di Fisica Nucleare, Sezione di Padova-Trento, [y]University of Padova, I-35131 Padova, Italy
[45]LPNHE, Universite Pierre et Marie Curie/IN2P3-CNRS, UMR7585, Paris, F-75252 France
[46]University of Pennsylvania, Philadelphia, Pennsylvania 19104
[47]Istituto Nazionale di Fisica Nucleare Pisa, [z]University of Pisa,
[aa]University of Siena and [bb]Scuola Normale Superiore, I-56127 Pisa, Italy
[48]University of Pittsburgh, Pittsburgh, Pennsylvania 15260
[49]Purdue University, West Lafayette, Indiana 47907
[50]University of Rochester, Rochester, New York 14627
[51]The Rockefeller University, New York, New York 10021
[52]Istituto Nazionale di Fisica Nucleare, Sezione di Roma 1,
[cc]Sapienza Università di Roma, I-00185 Roma, Italy
[53]Rutgers University, Piscataway, New Jersey 08855
[54]Texas A&M University, College Station, Texas 77843
[55]Istituto Nazionale di Fisica Nucleare Trieste/Udine,
I-34100 Trieste, [dd]University of Trieste/Udine, I-33100 Udine, Italy
[56]University of Tsukuba, Tsukuba, Ibaraki 305, Japan
[57]Tufts University, Medford, Massachusetts 02155
[58]Waseda University, Tokyo 169, Japan
[59]Wayne State University, Detroit, Michigan 48201
[60]University of Wisconsin, Madison, Wisconsin 53706
[61]Yale University, New Haven, Connecticut 06520

We present the first direct measurement of the W production charge asymmetry as a function of the W boson rapidity y_W in $p\bar{p}$ collisions at $\sqrt{s} = 1.96$ TeV. We use a sample of $W \to e\nu$ events in data from 1 fb^{-1} of integrated luminosity collected using the CDF II detector. In the region $|y_W| < 3.0$, this measurement is capable of constraining the ratio of up and down quark momentum distributions in the proton more directly than in previous measurements of the asymmetry that are a function of the charged-lepton pseudorapidity.

PACS numbers: 13.38.Be, 13.85.Qk, 14.60.Cd, 14.70.Fm

[*]Deceased

[†]With visitors from [a]University of Massachusetts Amherst,

At the Fermilab Tevatron, where $p\bar{p}$ collisions are produced at $\sqrt{s} = 1.96$ TeV, $W^+(W^-)$ bosons are created primarily by the interaction of u (d) quarks from the proton and $\bar{d}$ ($\bar{u}$) quarks from the anti-proton. Since u quarks carry, on average, a higher fraction of the proton's momentum than d quarks [1, 2], the W^+ tends to be boosted along the proton beam direction and the W^- tends to be boosted along the anti-proton direction. The difference between the W^+ and W^- rapidity distributions results in a charge asymmetry

$$A(y_W) = \frac{d\sigma/dy_{W^+} - d\sigma/dy_{W^-}}{d\sigma/dy_{W^+} + d\sigma/dy_{W^-}}, \quad (1)$$

where y_W is the W boson rapidity [3] and $d\sigma/dy_{W^\pm}$ is the differential cross section for W^+ or W^- boson production. The parton distribution functions (PDFs) describing the internal structure of the proton are constrained by measuring $A(y_W)$ [4].

Previous measurements [5–7] of the W charge asymmetry at the Tevatron were made as a function of the pseudorapidity η [3] of the leptons from decays of $W \to l\nu_l$ ($l = e, \mu$) since the W decay involves a neutrino whose longitudinal momentum is not determined experimentally. However, the lepton charge asymmetry is a convolution of the W production charge asymmetry and the $V - A$ asymmetry from W decays. These two asymmetries tend to cancel at large pseudorapidities ($|\eta| \gtrsim 2.0$), and the convolution weakens and complicates the constraint on the proton PDFs.

In the measurement presented in this Letter, the complication is resolved by using additional information in E_{T} and $\not\!\!E_{\mathrm{T}}$ [3] on an event-by-event basis to measure the asymmetry as a function of the $|y_W|$ instead of the lepton $|\eta|$. This gives the first direct measurement of the W production charge asymmetry using $W \to e\nu$ decays. The measurement uses data from 1 fb^{-1} of integrated luminosity collected by the CDF II detector, and employs a new analysis technique [8] that resolves the kinematic ambiguity of the event reconstruction by constraining the $e\nu$ mass to that of the W, thus allowing reconstruction of the W rapidity. The region of acceptance is $|y_W| < 3.0$, giving the new measurement an ability to improve proton PDFs determinations for $0.002 \lesssim x \lesssim 0.8$, where x is the fraction of the proton momentum carried by u- or d-type quarks.

The CDF II detector is described in detail elsewhere [9]. What follows is a brief description of the detector components needed to identify $W \to e\nu$ events, which are characterized by the presence of a large missing transverse energy ($\not\!\!E_{\mathrm{T}}$) and a track in the central drift chamber (COT) [10] or in the silicon tracking system (SVX) [11, 12] that points to a cluster of energy in the electromagnetic (EM) calorimeters [13, 14]. The SVX provides precise track measurements from eight radial layers of microstrip sensors. The COT provides additional tracking information from 96 layers of wires. Tracks are measured inside a 1.4 T solenoidal magnetic field that allows electron charge determination from the curvature of the track. The COT allows track reconstruction in the range $|\eta| \lesssim 1.6$, while the SVX extends the capability up to $|\eta| \simeq 2.8$. Outside the tracking system, EM and hadronic (HAD) calorimeters measure the energies of showering particles. The calorimeters are divided into two types: a central calorimeter with a fiducial region covering $|\eta| < 1.1$, and a forward calorimeter covering $1.2 < |\eta| < 3.5$.

We use two types of $W \to e\nu$ events, classified by the calorimeter section in which the electron is detected. The data are initially selected by an online event selection (trigger) system. The trigger for the central electrons requires an EM energy cluster with $E_{\mathrm{T}} > 18$ GeV and a matching track with $p_{\mathrm{T}} > 9$ GeV. The forward trigger, designed specifically for W candidates, requires an EM energy cluster with $E_{\mathrm{T}} > 20$ GeV and $\not\!\!E_{\mathrm{T}} > 15$ GeV. Additional requirements are made off line to distinguish electrons from photons and from quark and gluon jets.

For central electrons, we require off line event selection including an isolated energy cluster in the region $|\eta| < 1.1$ with $E_{\mathrm{T}} > 25$ GeV and Iso(0.4) < 4.0 GeV. The isolation Iso(0.4) is defined as the calorimeter energy contained within a cone of radius $R = \sqrt{(\Delta\eta)^2 + (\Delta\phi)^2} = 0.4$ [3] around the electron direction excluding the energy associated with the electron. We also require that a track must point to the central cluster with a ratio of cluster energy to track momentum (E/p) less than 2.0. A more detailed description of the central electron selection can be found in [15]. The forward electrons are selected by requiring an isolated energy cluster with $E_{\mathrm{T}} > 20$ GeV, the ratio of energy detected in the HAD and EM calorimeters to be less than 0.05, and an associated high quality track to re-

Amherst, Massachusetts 01003, [b]Universiteit Antwerpen, B-2610 Antwerp, Belgium, [c]University of Bristol, Bristol BS8 1TL, United Kingdom, [d]Chinese Academy of Sciences, Beijing 100864, China, [e]Istituto Nazionale di Fisica Nucleare, Sezione di Cagliari, 09042 Monserrato (Cagliari), Italy, [f]University of California Irvine, Irvine, CA 92697, [g]University of California Santa Cruz, Santa Cruz, CA 95064, [h]Cornell University, Ithaca, NY 14853, [i]University of Cyprus, Nicosia CY-1678, Cyprus, [j]University College Dublin, Dublin 4, Ireland, [k]University of Edinburgh, Edinburgh EH9 3JZ, United Kingdom, [l]University of Fukui, Fukui City, Fukui Prefecture, Japan 910-0017 [m]Kinki University, Higashi-Osaka City, Japan 577-8502 [n]Universidad Iberoamericana, Mexico D.F., Mexico, [o]Queen Mary, University of London, London, E1 4NS, England, [p]University of Manchester, Manchester M13 9PL, England, [q]Nagasaki Institute of Applied Science, Nagasaki, Japan, [r]University of Notre Dame, Notre Dame, IN 46556, [s]University de Oviedo, E-33007 Oviedo, Spain, [t]Texas Tech University, Lubbock, TX 79609, [u]IFIC(CSIC-Universitat de Valencia), 46071 Valencia, Spain, [v]University of Virginia, Charlottesville, VA 22904, [w]Bergische Universität Wuppertal, 42097 Wuppertal, Germany, [ee]On leave from J. Stefan Institute, Ljubljana, Slovenia,

duce the charge misidentification. In the region $|\eta| < 1.6$ tracks are reconstructed using COT information, while at higher $|\eta|$ tracks are reconstructed using the SVX detectors alone. In order to reduce the charge misidentification and backgrounds, additional E/p requirements for the forward tracks are imposed ($0.2 < E/p < 4.0$ for $1.2 < |\eta| < 1.6$ and $0.65 < E/p < 4.0$ for $|\eta| > 1.6$) and the extrapolated charged-particle position must be consistent with the position measured in the calorimeter. Candidate $W \to e\nu$ events are required to have exactly one $e^{\pm}$ candidate as well as $\not{E}_{\mathrm{T}} > 25$ GeV. The final $W \to e\nu$ data sample contains 537,858 events with a central electron and 176,941 forward electron events. To evaluate the detector acceptance and resolution for $W \to e\nu$ events we use the PYTHIA [19] event generator followed by the CDF detector simulation.

We determine the neutrino's longitudinal momentum, within a two-fold ambiguity, by constraining the $e\nu$ mass to be that of the W boson. This ambiguity can be resolved on a statistical basis from the known $V - A$ decay distribution using the decay angle between the electron and the proton in the W rest frame, θ^*, and from the W^+ and W^- production cross sections as a function of W rapidity ($d\sigma/dy_{W^{\pm}}$). To do this we assign a weighting factor to the two rapidity solutions, depending on the charge of the W boson, $w^{\pm}_{1,2}$:

$$w^{\pm}_{1,2} = \frac{P_{\pm}(\cos\theta^*_{1,2}, y_{1,2}, p_T^W)\sigma(y_{1,2})}{P_{\pm}(\cos\theta^*_1, y_1, p_T^W)\sigma(y_1) + P_{\pm}(\cos\theta^*_2, y_2, p_T^W)\sigma(y_2)}, \tag{2}$$

where

$$P_{\pm}(cos\theta^*, y_W, p_T^W) = (1 \mp cos\theta^*)^2 + Q(y_W, p_T^W)(1 \pm cos\theta^*)^2, \tag{3}$$

The $\pm$ signs indicate the W boson charge and the indices 1 and 2 are for the two W rapidity solutions. The differential cross section as a function of y_W is determined using a next-to-next-to-leading order (NNLO) QCD calculation [16]. The ratio of the $(1+\cos\theta^*)^2$ to $(1-\cos\theta^*)^2$ angular distributions, $Q(y_W, p_T^W)$, in Eq. 3 is determined by the quark versus anti-quark composition of the proton at next-to-leading order (NLO) using the event simulation generator MC@NLO [17]. This ratio is evaluated as a function of y_W and the W transverse momentum p_T^W. The parameters of this weighting factor are determined using CTEQ6.1 PDF set [18], and their dependence on the input PDFs is evaluated as a source of systematic uncertainty. Although the weighting factor given by Eq. 2 depends primarily on the W^+ and W^- cross sections, it does have some weak dependence on the assumed W charge asymmetry. Therefore, this method requires us to iterate the procedure to eliminate the dependence on the input asymmetry.

Correct charge identification is crucial for the measurement of the charge asymmetry measurement, because it directly affects the yield for a particular charge and y_W. The charge misidentification rate (Charge MisID) is measured as a function of η using $Z \to ee$ events where both electrons are identified as having the same charge sign. The misidentification rate ranges from $(0.18 \pm 0.05)\%$ for $|\eta| < 1.1$ to $(17.26 \pm 2.02)\%$ for $|\eta| > 2.04$. The effect of the charge misidentification is corrected for on an event-by-event basis.

The $A(y_W)$ values are corrected for the backgrounds to $W \to e\nu$ candidates. We consider $W \to \tau\nu$, where the τ decays leptonically to an electron plus neutrinos, as contributing to the signal. It is included in the overall signal acceptance, with central and forward electron contributions of $(2.30 \pm 0.04)\%$ and $(2.04 \pm 0.05)\%$, respectively. The background fractions due to $Z \to e^+e^-$ events where one of the electrons is not reconstructed and mimics a neutrino are $(0.59 \pm 0.02)\%$ for central electrons and $(0.54 \pm 0.03)\%$ for forward electrons. The small contamination from the $Z \to \tau^+\tau^-$ process is found to be $(0.10 \pm 0.01)\%$ for both central and forward electrons. The background from misidentified jets (QCD) is estimated by fitting the isolation distribution of electrons. Electrons in the calorimeter are characterized by having most of their energy deposited within an isolation cone centered on the electron, while jets may have significant energy deposits outside this cone. The QCD background fraction for central and forward electrons are $(1.21 \pm 0.21)\%$ and $(0.67 \pm 0.18)\%$, respectively.

The scale and resolution of the electromagnetic calorimeter energy and the missing transverse energy can affect the measured W rapidity and thus the asymmetry measurement. The EM calorimeter energy scale and resolution are tuned in the simulation to reproduce the $Z \to e^+e^-$ mass peak observed in data. The uncertainties on the energy scale and resolution for central electrons are measured to be $\pm$ 0.05% and $\pm$ 0.07%; for forward electrons they are $\pm$ 0.3% and $\pm$ 0.8%, respectively. The hadronic showering, the boson recoil-energy, and the underlying event energy of the hadronic calorimeter energy measurement play important roles in determining the $\not{E}_{\mathrm{T}}$. The simulation for the calorimeter deposition in $W \to e\nu$ events is tuned to provide the best possible match with data, including its dependence on η. The uncertainty on the transverse recoil energy scale is $\pm$ 0.3% and $\pm$ 1.4% for central and forward electrons, respectively.

We also investigate potential sources of a charge bias and η dependence in the kinematic and geometrical acceptance of the event (estimated with simulated data) and efficiencies of the trigger and the electron identification (measured with data). The trigger efficiencies for the central and forward electrons are measured using data from independent triggers. We find the trigger efficiencies do not depend on charge, but do depend on the η and E_{T} of the electron. The average trigger efficiencies for the central and forward electrons are $(96.1 \pm 1.0)\%$ and $(92.5 \pm 0.3)\%$, respectively. Electron identification

TABLE I: Statistical and systematic uncertainties for the W production charge asymmetry. All values are ($\times 10^{-2}$) and show the correlated uncertainties for both positive and negative rapidities.

$\|y_W\|$	Charge MisID	Back-grounds	Energy Scale & Resolution	Recoil Model	Electron Trigger	Electron ID	PDFs	Stat.
0.0 - 0.2	0.02	0.04	0.01	0.11	0.03	0.02	0.03	0.31
0.2 - 0.4	0.01	0.09	0.04	0.22	0.08	0.07	0.08	0.32
0.4 - 0.6	0.02	0.11	0.06	0.22	0.13	0.17	0.15	0.33
0.6 - 0.8	0.03	0.15	0.07	0.34	0.14	0.30	0.22	0.32
0.8 - 1.0	0.03	0.20	0.07	0.42	0.11	0.47	0.24	0.34
1.0 - 1.2	0.04	0.18	0.08	0.33	0.09	0.69	0.27	0.38
1.2 - 1.4	0.05	0.18	0.15	0.67	0.06	0.78	0.28	0.43
1.4 - 1.6	0.04	0.14	0.14	1.10	0.04	0.85	0.28	0.50
1.6 - 1.8	0.08	0.12	0.26	0.92	0.03	0.89	0.29	0.55
1.8 - 2.05	0.22	0.13	0.31	0.82	0.06	0.80	0.34	0.62
2.05 - 2.3	0.44	0.21	0.53	0.59	0.17	0.85	0.42	0.83
2.3 - 2.6	0.45	0.19	0.62	0.40	0.27	0.86	0.50	1.10
2.6 - 3.0	0.14	0.10	0.60	0.43	0.28	0.65	0.53	2.30

and track matching efficiencies (ID) are measured in data and simulation using the $Z \to e^+e^-$ channel. We correct $W \to e\nu$ simulated events by the ratio of the efficiencies in control data and simulation.

The choice of PDF sets has an effect on the shape of the $d\sigma^{\pm}/dy_W$ distribution, as well as on the ratio of quarks and anti-quarks in the angular decay distribution. We use the 40 CTEQ6.1 error PDF sets and re-determine the $d\sigma^{\pm}/dy_W$ production cross section and the angular distribution of $\cos\theta^*$ for each error PDF set. The PDFs uncertainties on the W charge asymmetry are evaluated using the 40 CTEQ6.1 eigenvectors with 90% C.L. variations and are summed in quadrature.

As expected, the data are found to be invariant under CP transformations $A(y_W) = -A(-y_W)$, the two sets of points are in statistical agreement, so we combine the $A(y_W)$ bins with the complementary $-A(-y_W)$ bins in order to improve the precision of the measurement of the asymmetry. We quote the statistical combination of the asymmetry at positive rapidity with the negative value of the asymmetry at negative rapidity, using the Best Linear Unbiased Estimate (BLUE) method [20], accounting for all correlations for both positive and negative bins in W rapidity. The statistical correlation coefficient between bins is evaluated using pseudo-experiments and is found to be < 0.05. Table I summarizes the statistical and systematic uncertainties on $A(|y_W|)$.

The measured asymmetry $A(|y_W|)$, which combines the positive and negative y_W bins, is shown in Fig. 1. Also shown are the predictions of a NNLO QCD calculation using the MRST 2006 NNLO PDF sets [21] and a NLO QCD calculation using the CTEQ6.1 NLO PDF sets. Values of $A(y_W)$ for each $|y_W|$ bin with the total uncertainty obtained in this measurement are listed in Table II, where the bin centers are defined to account for the W rapidity and mass acceptance in each bin, by averaging the W rapidity using the weighted W data. Since this measurement depends on the width of the W, in particular for the highest y_W bin, we use our simulated data to estimate the charge asymmetries both in the W-mass range accepted for each bin, and for a fixed W mass ($m_W = 80.403$ GeV/c^2). The bin centers in Table II are corrected to the value of $<|y_W|>$ for which the asymmetry is equal to the one at $m_W = 80.403$ GeV/c^2. In conclusion, using a new analysis technique, we report the

TABLE II: The W production charge asymmetry with total systematic and statistical uncertainties. The average $<|y_W|>$ indicates an average value of W^+ and W^- rapidity in each y_W bin and at a fixed W mass, $m_W = 80.403$ GeV/c^2.

$\|y_W\|$	$<\|yW\|>$	$A(y_W)$	σ_{sys}	$\sigma_{sys+stat}$
0.0 - 0.2	0.10	0.020	±0.001	±0.003
0.2 - 0.4	0.30	0.057	±0.003	±0.004
0.4 - 0.6	0.50	0.081	±0.004	±0.005
0.6 - 0.8	0.70	0.117	±0.006	±0.006
0.8 - 1.0	0.89	0.146	±0.007	±0.008
1.0 - 1.2	1.09	0.204	±0.008	±0.010
1.2 - 1.4	1.29	0.235	±0.011	±0.012
1.4 - 1.6	1.49	0.261	±0.014	±0.015
1.6 - 1.8	1.69	0.303	±0.014	±0.014
1.8 - 2.05	1.91	0.355	±0.013	±0.014
2.05 - 2.3	2.15	0.436	±0.013	±0.016
2.3 - 2.6	2.40	0.537	±0.014	±0.018
2.6 - 3.0	2.63	0.642	±0.012	±0.026

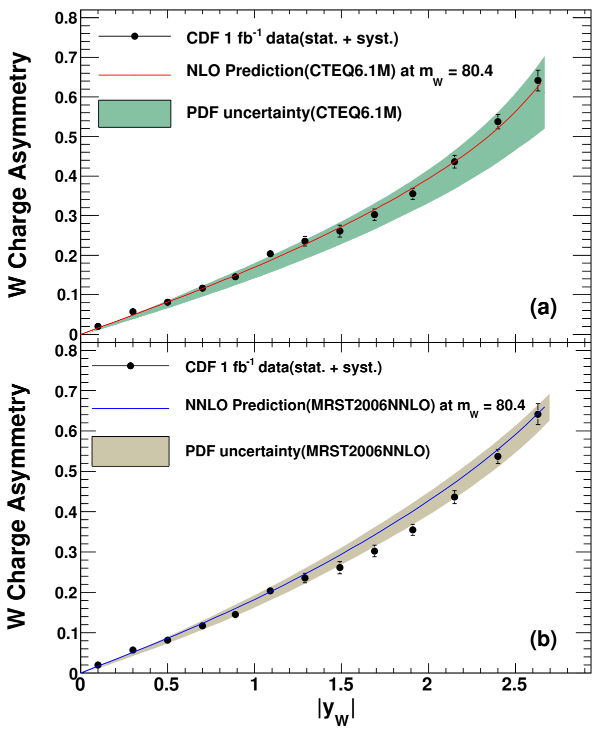

FIG. 1: The measured W production charge asymmetry and predictions from (a) NLO CTEQ6.1 with the associated PDFs uncertainty and (b) NNLO MRTST2006 and its associated PDFs uncertainty.

first direct measurement of the W boson charge asymmetry from Run II of the Tevatron, using data from 1 fb^{-1} of integrated luminosity taken with the CDF II detector. Since the total uncertainties are smaller than the uncertainties coming from PDFs, as is also shown in [8], this measurement should significantly improve the sensitivity on the ratio of d/u momentum distributions in the proton over previous lepton charge asymmetry measurements at the Tevatron. This result is therefore expected to improve the precision of the global PDFs fits.

We wish to thank R.S. Thorne and W.J. Stirling for useful discussions on the theoretical predictions. We thank the Fermilab staff and the technical staffs of the participating institutions for their vital contributions. This work was supported by the U.S. Department of Energy and National Science Foundation; the Italian Istituto Nazionale di Fisica Nucleare; the Ministry of Education, Culture, Sports, Science and Technology of Japan; the Natural Sciences and Engineering Research Council of Canada; the National Science Council of the Republic of China; the Swiss National Science Foundation; the A.P. Sloan Foundation; the Bundesministerium für Bildung und Forschung, Germany; the Korean Science and Engineering Foundation and the Korean Research Foundation; the Science and Technology Facilities Council and the Royal Society, UK; the Institut National de Physique Nucleaire et Physique des Particules/CNRS; the Russian Foundation for Basic Research; the Ministerio de Ciencia e Innovación, and Programa Consolider-Ingenio 2010, Spain; the Slovak R&D Agency; and the Academy of Finland.

---

[1] A.D. Martin, W.J. Stirling, R.G. Roberts, Phys. Rev. D **50**, 6734 (1994).

[2] H.L. Lai *et al.*, Phys. Rev. D **51**, 4763 (1995).

[3] We assume a (z, ϕ, θ) coordinate system with the z-axis in the direction of the proton beam; ϕ and θ are the azimuthal and polar angle respectively. The rapidity (y_W) and pseudorapidity (η) are defined as $y_W = ln\frac{E+P_z}{E-P_z}$ and $\eta = -ln(\tan\frac{\theta}{2})$, and the transverse momentum and energy as $p_T = p\sin\theta$ and $E_T = E\sin\theta$, respectively. Missing transverse energy, $\not{E}_T = |\vec{\not{E}}_T|$, is defined as $\vec{\not{E}}_T = -\sum_i E^i_T \hat{\mathbf{n}}_\mathbf{i}$ where $\hat{\mathbf{n}}_\mathbf{i}$ is the component in the transverse plane of a unit vector that points from the interaction point to the i^{th} calorimeter tower.

[4] E. L. Berger, F. Halzen, C.S. Kim, and S. Willenbrock, Phys. Rev. D **40**, 83 (1989); **40**, 3789 (1989).

[5] F. Abe *et al.* (CDF Collaboration), Phys. Rev. Lett. **81**, 5754 (1998).

[6] V. M. Abazov *et al.* (D0 Collaboration), arXiv:0709.4254 [hep-ex], accepted by Phys. Rev. D Rapid Comm.

[7] D. Acosta *et al.* (CDF Collaboration), Phys. Rev. D **71**, 051104 (2005).

[8] A. Bodek, Y. Chung, B.-Y. Han, K. McFarland, E. Halkiadakis, Phys. Rev. D **77**, 111301(R) (2008).

[9] D. Acosta *et al.* (CDF Collaboration), Phys. Rev. D **71**, 032001 (2005).

[10] T. Affolder *et al.* (CDF Collaboration), Nucl. Instrum. Methods Phys. Res., Sect. A **526**, 249 (2004).

[11] A. Sill *et al.* (CDF Collaboration), Nucl. Instrum. Methods Phys. Res., Sect. A **447**, 1 (2000).

[12] A. Affolder *et al.* (CDF Collaboration), Nucl. Instrum. Methods Phys. Res., Sect. A **453**, 84 (2000).

[13] L. Balka *et al.* (CDF Collaboration), Nucl. Instrum. Methods Phys. Res., Sect. A **267**, 272-279 (1988).

[14] M. Albrow *et al.* (CDF Collaboration), Nucl. Instrum. Methods Phys. Res., Sect. A **480**, 524-545 (2002).

[15] A. Abulencia *et al.* (CDF collaboration), J. Phys. G: Nucl. Part. Phys. **34**, 2457 (2007).

[16] C. Anastasiou, L. Dixon, K. Melnikov, F. Petriello, Phys. Rev. D **69**, 094008 (2004).

[17] S. Frixione and B.R. Webber, J. High Energy Phys. **0206** 029 (2002); S. Frixione, P. Nason and B.R. Webber, J. High Energy Phys. **0308** 007.

[18] J. Pumplin, D.R. Stump, J. Huston, H.L. Lai, S. Kuhlmann, J.F. Owens and W.K. Tung, J. High Energy Phys. **0310**, 046 (2003).

[19] T. Sjöstrand *et al.*, Comp. Phys. Comm. **135**, 238 (2001).

[20] L. Lyons, D. Gibaut, and P. Clifford, Nucl. Instrum. Methods Phys. Res., Sect. A **270**, 110 (1988).

[21] A.D. Martin, W.J. Stirling, R.S. Thorne and G. Watt, Phys. Lett. B **652** 292 (2007).